Nanostructured materials based on the integration of ferrocenyl-tethered dendrimer and redox proteins on self-assembled monolayers: an efficient biosensor interface

2009 Nanotechnology 20 505501

(http://iopscience.iop.org/0957-4484/20/50/505501)

Nanotechnology **20** (2009) 505501 (8pp) doi:10.1088/0957-4484/20/50/505501

Nanostructured materials based on the integration of ferrocenyl-tethered dendrimer and redox proteins on self-assembled monolayers: an efficient biosensor interface

Marco Frasconi[1], **Daniela Deriu**[1], **Andrea D'Annibale**[2] and **Franco Mazzei**[1,3]

[1] Department of Chemistry and Drug Technologies, Sapienza University of Rome, Piazzale Aldo Moro, 500185 Rome, Italy
[2] Department of Chemistry, Sapienza University of Rome, Piazzale Aldo Moro, 500185 Rome, Italy

E-mail: franco.mazzei@uniroma1.it

Received 16 July 2009, in final form 19 October 2009
Published 12 November 2009
Online at stacks.iop.org/Nano/20/505501

Abstract

In this paper we report the use of ferrocenyl-tethered dendrimer (Fc-D) as an electrode modifier supported by a self-assembled monolayer coated gold surface. The pretreatment of electrodes with Fc-D allows the covalent immobilization of glucose oxidase. The resulting integrated hybrid system provides electrical contact between the redox center of the enzyme and the electrode, and improves the overall bioelectrocatalyzed oxidation of glucose. Cyclic voltammetry combined with surface plasmon resonance (SPR) is used to investigate the redox-induced orientation changes of ferrocene-tethered dendrimers and the optimal electrical wiring of the enzyme, depending on the length of the alkyl chain of the ferrocene-tethered groups. The amount of substrate controls the steady-state concentration ratio of Fc/Fc^+ in the film composition. Therefore, the SPR spectrum of the film is controlled by the reversible change in the refractive index of the enzyme-integrated redox film. The proposed method demonstrates a new procedure for developing a stable amperometric redox enzyme-based sensor by designing a new nanostructured material that control the biosensing performance.

(Some figures in this article are in colour only in the electronic version)

1. Introduction

The structural organization and electron transfer function of chemical and biological redox molecules on solid surfaces are hugely relevant in nano-biotechnology, which combines physical and chemical nanoscale science and biotechnological aspects. Electrochemical investigation of the electron transfer kinetics of redox enzymes immobilized on conductive surfaces has been recognized to be a powerful approach for better understanding of long-range electron transfer, which is one of the fundamental processes occurring in nature [1, 2]. The electrical communication between redox enzymes and electronic transducers is also one of the most challenging topics in bioelectronics [3], with important implications for the development of electrochemical biosensors [4, 5] and biofuel cell elements [6, 7]. The direct electron transfer approach to proteins requires interfaces that exhibit fast electron transfer kinetics and immobilization procedures able to retain their redox and biocatalytic properties. Since direct contact between redox enzymes and electrode surfaces leads to significant structural and functional changes in the enzyme [8], in the past

[3] Author to whom any correspondence should be addressed.

couple of decades numerous strategies have been developed to promote efficient electron exchange between the electrode surface and immobilized redox proteins. The development of diffusional electron mediators [9], the tethering of the redox-active unit to the enzyme [10–12], the immobilization of biocatalysts in redox-active polymers [13, 14] or the surface reconstitution of redox apo-enzymes on relay cofactor units [15–17] provide general routes to enzyme–electrode communication. Both conductive and functionalized polymers have been applied as wiring matrices for the electrochemical activation of redox enzymes; for instance, an Os complex-containing polymer provides an oxidative electron path for entrapped glucose oxidase [13, 18], whereas a bipyridinium-containing polymer allows reductive electron transfer to the nitrate reductase enzyme [19].

Thus, it appears that the key issue for investigate the redox processes of enzymes at electrode surfaces is to design a biocompatible interface that is able to preserve the immobilized protein from structural and functional changes, allowing accurate control over the distance between the redox center of the protein and the electrode surface. Among the protein immobilization strategies able to achieve these criteria, the method based on highly branched polymers called 'dendrimers' has been recently recognized as a promising candidate building unit to obtain highly ordered bionanostructured materials [20, 21]. The peculiar properties of metallocenyl dendrimers, such as the high number of functionalized groups and their versatility, make them an interesting source for producing nanostructured materials for applications in molecular electronics, catalysis and chemical/biological sensing [22–26]. Moreover, efficient and fast electrochemical communication between the redox centers immobilized on the outside edge of the dendrimer has been observed [23, 27, 28]. In order to develop optimized electron transfer based biosensors, dendrimer immobilization on the electrode surface is a crucial step in ensuring efficient communication between redox protein-bound dendrimer and the transducer surface. In this regard, film formation on a self-assembled monolayer (SAM) is an appealing choice for immobilizing sensing molecules on the transducer surface [29, 30].

In this work we employed SAM technology to realize nanostructured films consisting of fourth generation poly(amidoamine) dendrimers (G4 PAMAM) for the covalent immobilization of both electron transfer mediator units (ferrocene) and the enzyme glucose oxidase as components of an electrochemical biosensor. In order to obtain high performing biodevices, we studied the following issues by means of the *in situ* electrochemical surface plasmon resonance (EC-SPR) technique: (a) the nature and the strength of the interaction between the surface and the functionalized dendrimers, (b) the stability of the resulting films, and (c) the optimal electrical wiring of the enzyme, in terms of the length of the alkyl chain of the ferrocene-tethered groups. The coupling of surface plasmon resonance with electrochemistry (EC-SPR) provides a viable possibility for simultaneously probing the optical and electrochemical properties of adsorbate films at the metal/solution interface and sensitive detection of variation in the thin films thickness accompanying redox reactions [31–33]. Only a few examples of *in situ* EC-SPR measurements in the presence of redox proteins are available in literature [15, 34].

Herein EC-SPR measurements revealed the redox-induced orientation changes of ferrocene-tethered dendrimers. We also demonstrate that SPR spectroscopy may be employed as a complementary method to electrochemistry to transduce the bioelectrocatalytic transformations.

2. Experimental details

2.1. Reagents and materials

All the chemicals used were of analytical grade from Sigma-Aldrich without further purification. 11-amino-1-undecanethiol (AUT; >99% purity) was purchased from Dojindo Laboratories (Kumamoto, Japan). All aqueous solutions were prepared using deionized water (specific resistivity $\geqslant$18.2 MΩ cm) obtained from a Direct-Q 3 UV apparatus (Millipore, France). All solvents used in monolayer preparation were of p.a. grade.

Glucose oxidase (EC 1.1.3.4., type VII-S, from *Aspergillus niger*) was used as-received from Sigma. Carbohydrate groups on the peripheral surface of the glucose oxidase (GOx) molecules were oxidized as described in the literature [35, 36]. For this reaction, to a 20 μM GOx solution (5 ml of 0.1 M phosphate buffer pH 6.8), 30 mg of sodium periodate was added, and the obtained solution was stirred for 1 h at 4 °C. The reaction was stopped with 25 mM ethylene glycol for 30 min at 25 °C, and the product was purified and concentrated with ultracentrifugation (molecular weight cutoff 30 000, Centricon).

Dialysis membranes (SpectraPorr 7 MWco 3.5 kDa) were purchased from Spectropore Europe.

2.2. Ferrocene-tethered dendrimer synthesis

*2.2.1. Synthesis of ferrocenyl-tethered PAMAM G4–NH_2 dendrimers Fc-D(**1**).* Primary amines of NH_2-terminated G4 PAMAM dendrimers were partially modified with ferrocenyl groups through the imine forming, amine–aldehyde reaction as previously reported [26]. Ferrocenemonocardoxaldehyde (0.52 mmol) was dissolved in methanol (4.0 ml) and the mixture was added to 0.25 ml of 10% (w/w) G4 PAMAM dendrimer solution containing hydrochloric acid as a catalyst. The reaction mixture was stirred for 2 h, and 5 mg of sodium borohydride was slowly added and stirred for 1 h to reduce carbon-to-nitrogen double bonds. The reaction product was purified by lipophilic gel permeation chromatography (Sephadex LH-20, Pharmacia) using methanol as the eluant.

*2.2.2. Synthesis of ferrocenyl-tethered PAMAM G4–NH_2 dendrimers Fc-D(**2**).* Synthesis of 12-ferrocenyldodecanoic acid has been developed according a procedure reported in the literature [37] starting from ferrocene, with slight modifications.

11-Ferrocenyldodecanonitrile (0.66 mmol) was dissolved in pure ethanol (5.0 ml), aqueous KOH 5N (4.8 ml) was added and the mixture was refluxed for 10 h, then acidified with HCl

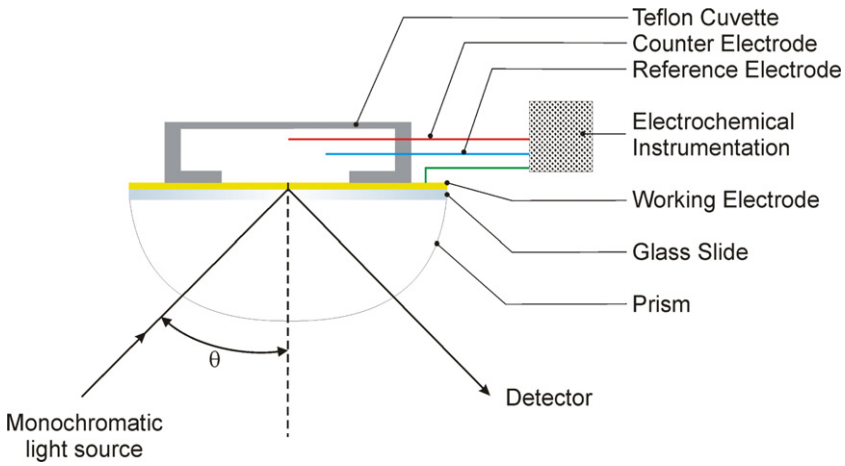

Scheme 1. Experimental set-up based on a surface plasmon resonance (SPR) spectrometer combined with an electrochemical module for the simultaneous characterization of structural and functional features of the modified gold surface.

(pH 2.0) and extracted with CH_2Cl_2 (3 × 20 ml). The organic layer was dried over Na_2SO_4, filtered and evaporated under vacuum. Ferrocenyldodecanoic acid (240 mg, 0.63 mmol, 95% yield) was recovered as a yellow solid.

12-Ferrocenyldodecanoic acid (0.59 mmol) was dissolved in DMSO (9 ml) and DCC (206 mg, 1 mmol) was added as a coupling agent with stirring; then PAMAM G4-NH_2 (147 mg, 0.01 mmol) dissolved in DMSO (4.0 ml) was added and the mixture was stirred at 25 °C for 4 days. The solvent was removed with a distillation under vacuum and the residue (160 mg) was dissolved in MeOH and purified with dialysis against MeOH to afford 140 mg of product.

2.3. In situ electrochemical SPR measurements

A surface plasmon resonance (SPR) Kretschmann type spectrometer [38], Autolab Esprit (Eco Chemie, Utrecht, The Netherlands), with an LED light source with an emission wave of 670 nm and a prism refraction index of 1.52 was used to perform the optical measurements of the SPR angle. In this configuration, the intensity of the reflected light is a minimum at the resonance angle. This angle can be measured over a range of 4° after focusing by a lens into a photodiode detector. The incident angle is varied by using a vibrating mirror (rotating over an angle of 5° at 77 Hz in 13 ms) with a resolution of 1 millidegree. The glass supported SPR substrates at the prism were clamped against a Teflon cuvette with O-rings, providing liquid-tight seals. An autosampler (Eco Chemie) with a controllable aspirating–dispensing–mixing pipette was used to add samples to the cuvette and provide a constant mixture by aspiration and dispensing during measurements. This experimental arrangement maintains a homogeneous solution and reproducible hydrodynamic conditions. The temperature of the cuvette was maintained at 25 ± 1 °C. Data were transmitted to a laptop computer and analyzed by SPR software version 4.1.2 from Eco Chemie.

A key role in the structural and functional characterization of the ferrocene-tethered dendrimer modified surface is played by the combined set-up of the SPR spectrometer and electrochemical instrument. The basic concept of this very powerful tool is schematically given in scheme 1. The classical SPR (shown in the Kretschmann configuration) is complemented by an μAutolab electrochemical analyzer (Eco Chemie, Utrecht, The Netherlands) in a three-electrode set-up. The gold SPR substrate at the prism mounted against the Teflon cell with use of an O-ring was used as a working electrode (0.8 mm^2 area exposed to the solution). The Teflon cell allowed for simultaneous recording of SPR and electrochemical data and application of a voltage to the sample. Auxiliary Pt and quasi-reference Ag electrodes made from wires of 0.5 nm diameter were part of the cell. The Ag quasi-reference electrode was calibrated according to the potential of dimethyl viologen (N,N'-dimethyl-4,4′-bipyridiniumdichloride) [39], $E^0 = -0.687$ V versus standard calomel electrode (SCE), measured by cyclic voltammetry, and the potentials are versus SCE.

2.4. Preparation of ferrocene-tethered dendrimer on self-assembled modified Au surfaces and the assembly of glucose oxidase

Glass supported gold substrates for SPR spectroscopy and electrochemistry, composed of a gold sensing surface (thickness 50 nm) deposited onto a glass microscope slide with a titanium adhesion layer (1.5 nm), were purchased from Xantec Bioanalytics (Muenster, Germany). The planar gold SPR disks were extensively cleaned in a freshly prepared piranha solution (3:1 H_2SO_4 98%: H_2O_2 30%). After 1 h the disks were thoroughly rinsed with ethanol, dried in a stream of nitrogen gas and immediately incubated overnight in 1 mM of 11-mercaptoundecanoic acid (MUA) in ethanol. After SAM formation, the disks were washed with ethanol and water, and dried with nitrogen gas.

For the detailed experiment, the MUA modified gold sensor disk was first placed onto the prism of the SPR system. The carboxyl functions on the SAM layer were activated with 5 mM EDC. After rinsing the disk, 1.5 μM aqueous solution of Fc-D ((**1**) or (**2**)) was flowed over the sensor surface for 1 h,

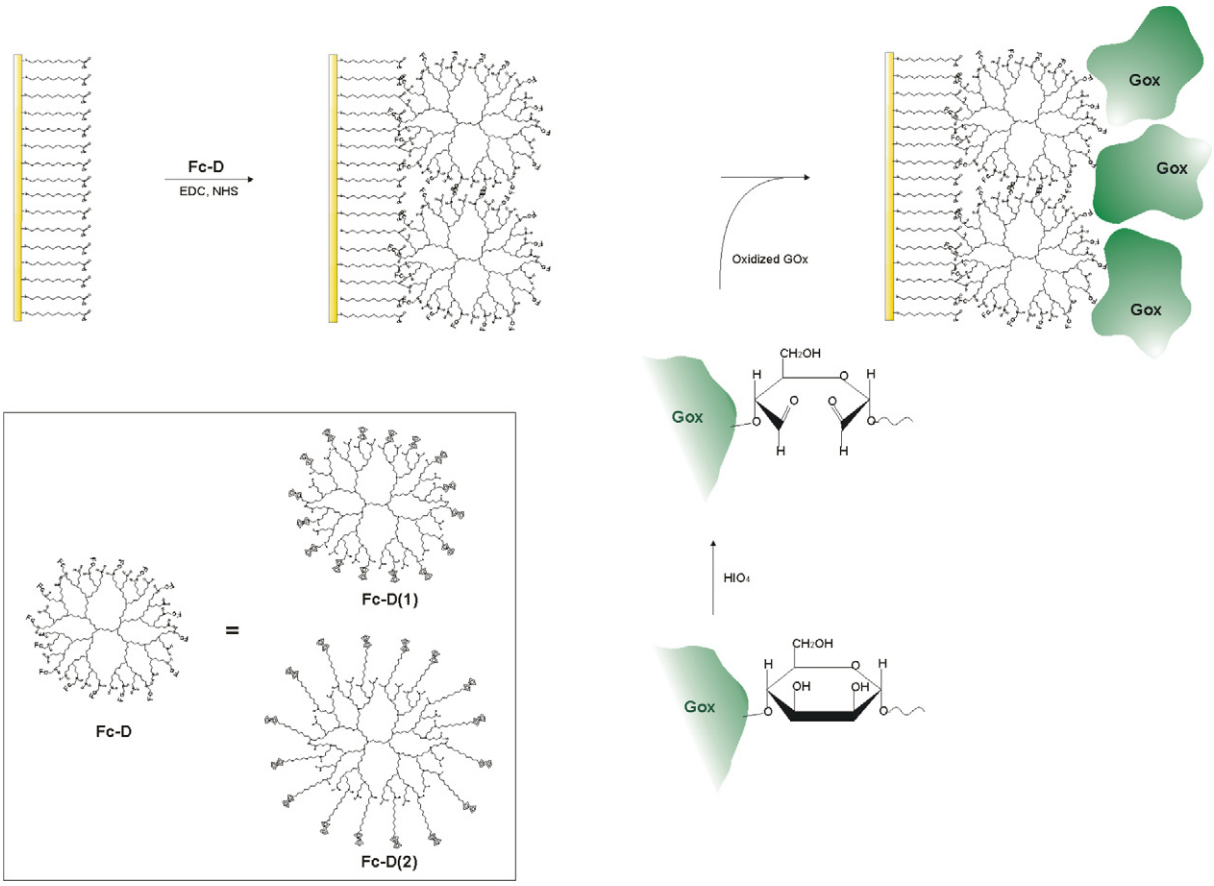

Scheme 2. Assembly of the integrated GOx ferrocenyl-tethered dendrimer (Fc-D) modified MUA SAM gold surface.

to achieve covalent cross-linking by amino reactive groups of the dendrimer with the aldehyde terminals. After washing, the modified surfaces were coated with 40 μM periodate-oxidized GOx solution in 0.1 M phosphate buffer (pH 6.8) for 1 h at 25 °C. The resulting integrated electrodes were used for the bioelectrocatalyzed detection of glucose.

3. Results and discussion

Scheme 2 outlines the method of preparation and assembly of the GOx ferrocene-tethered dendrimer on a gold electrode. A monolayer of MUA was assembled on the gold surface, and this acted as an anchoring base layer. The Fc-D was covalently linked to the functionalized electrode to yield the Fc-D modified MUA SAM surface. Voltammetric analysis of the Fc-D modified electrodes (figure 1(A)) showed a quasi-reversible redox wave at 0.288 ± 0.005 V versus SCE for the Fc-D(**1**) and at 0.295 ± 0.004 V versus SCE for Fc-D(**2**). Obviously, no voltammetric peaks were observed for the dendrimer modified MUA SAM surface in the same potential window. The anodic-to-cathodic peak current ratio of the Fc-D modified electrodes was close to unity, and a linear relationship between the scan rate and the current intensity was found (figure 1(A), inset), as expected for a surface-confined redox species [40]. Integration of the anodic peak, with correction for the charging current contribution, yielded the charge associated with the ferrocene oxidation; from this value a surface coverage (Γ) of 6.0×10^{-10} mol cm^{-2} and 6.6×10^{-10} mol cm^{-2} of the ferrocene units associated with Fc-D(**1**) and Fc-D(**2**), respectively, was evaluated. At a high scan rate ($v > 0.5$ V s^{-1}), the peak potential difference between the anodic and cathodic waves increased, reflecting progressive kinetic control by the rate of electron transfer of the ferrocene units (figure 1(B)). From the shift of the anodic and cathodic peak potentials as a function of the scan rate, the electron transfer rate constant (k_{ET}) was estimated using the Laviron method [41]. By using a ferrocene charge transfer coefficient (α) of 0.5, the best fit gave a k_{ET} value of 89 s^{-1} for Fc-D(**1**) and 51 s^{-1} for Fc-D(**2**). The observed decrease of k_{ET} suggests that the length of the linker between dendrimer and ferrocene units influences the electron transfer process on the electrode surface. Perhaps the most noteworthy findings that corroborate a different electron transfer mechanism for the two Fc-Ds are the magnitude of the SPR dip shifts (figure 2). As the potential is swept in the anodic direction, a sigmoidal increase in the SPR angle ($\Delta\theta$) is observed which begins to plateau before the sweep direction is reversed. The change of the SPR dip is rather fast, suggesting that the redox-induced reorganization is instantaneous. Although there is some hysteresis between the forward and reverse sweeps, in both cases the SPR angle returns approximately to its original value at the end of the cyclic voltammogram, suggesting that any redox-induced surface change is reversible.

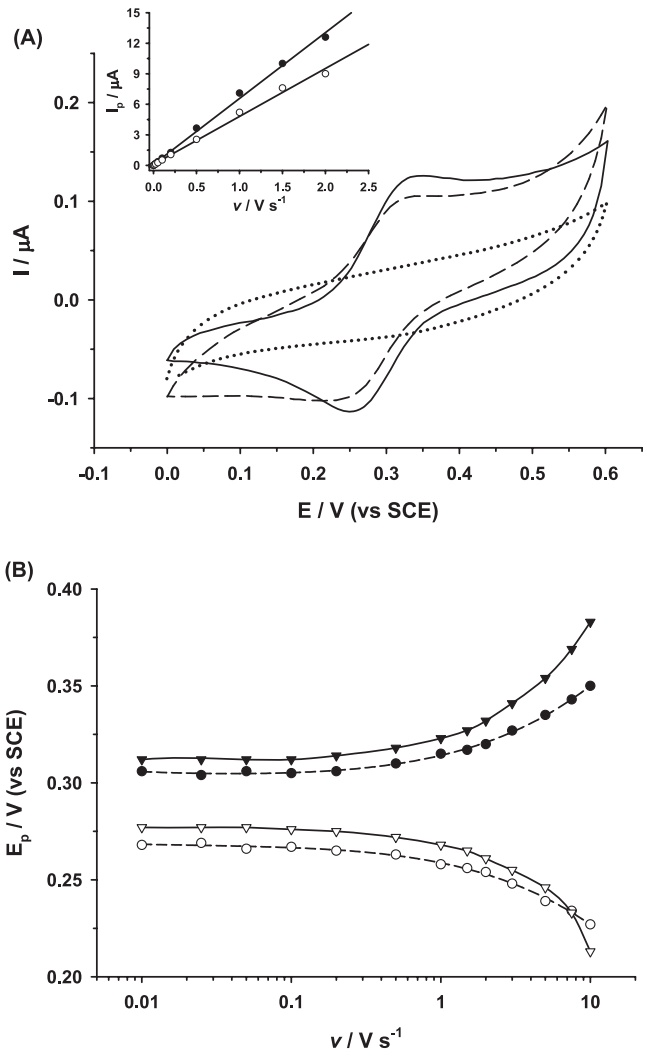

Figure 1. (A) Cyclic voltammograms of the dendrimer modified MUA SAM surface (dotted line) and Fc-D modified MUA SAM surfaces with a short (**1**, dashed line) and long (**2**, solid line) alkyl chain. Scan rate 0.01 V s^{-1}. Inset: variation of anodic peak intensities as a function of the scan rate for Fc-D(**1**) (empty circles) and Fc-D(**2**) (filled circles). The solid lines show the linear regression fitting. (B) Position of the anodic (filled symbols) and cathodic (empty symbols) peak potential as a function of the scan rate for Fc-D(**1**) and Fc-D(**2**). The dashed lines and the solid line show the theoretical curves calculated from the Laviron model for Fc-D(**1**) and Fc-D(**2**), respectively. The overall data were collected in 50 mM Tris-HCl buffer pH 7.2 and 50 mM KCl at 25 °C.

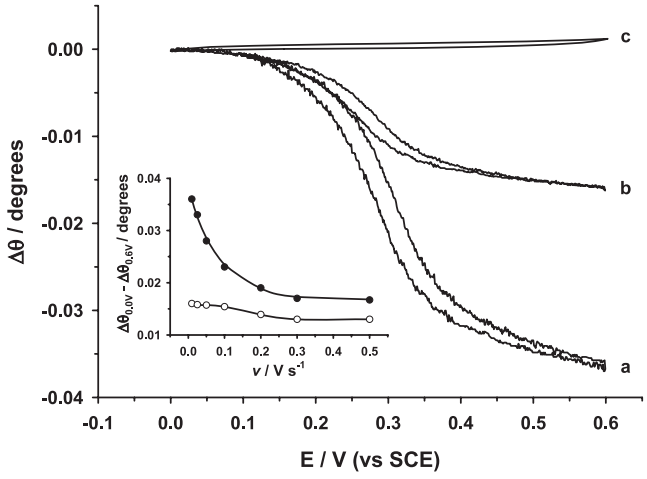

Figure 2. EC-SPR diagrams of Fc-D(**2**) (a), Fc-D(**1**) (b) and dendrimer (c) modified MUA SAM surfaces at 0.01 V s^{-1}. Inset: dependence of the SPR dip shift potential signals on the potential scan rate for Fc-D(**1**) (empty circles) and Fc-D(**2**) (filled circles). All measurements were performed in 50 mM Tris-HCl buffer pH 7.2 and 50 mM KCl.

The SPR angle potential shape for Fc-D(**1**) and Fc-D(**2**) are qualitatively similar, though it is clear that the magnitude of the angular changes is greater, by more than a factor 2, for Fc-D(**2**) than for Fc-D(**1**). To exclude the possible influence of the SPR dip shift on the change in the electron density of the electrode during the potential scan [42], an EC-SPR experiment was carried out at a dendrimer modified MUA SAM gold electrode. The change in the SPR dip shift in the anodic direction is nonsigmoidal and rather small (see curve c, figure 2), suggesting that the variation of the electron density of the underlying electrode would not cause an appreciable SPR dip shift. Implicit in the SPR angle potential profile is information relating to the kinetics of the redox-induced Fc-D reorganization. In general, the dependence of the SPR angular shift on an applied potential is predominantly regulated by three factors, namely electron density changes at the metal surface ($\Delta\sigma$), monolayer thickness changes (Δd) and refractive index changes (Δn), as reported in the equation below [43, 44]:

$$\frac{\Delta\theta_R(\lambda)}{\Delta V} = c_1\frac{\Delta n(\lambda)}{\Delta V} + c_2\frac{\Delta d}{\Delta V} + c_3\frac{\Delta\sigma}{\Delta V}$$

where c_1, c_2 and c_3 are system-dependent constants and λ is the wavelength of the incident light (constant in this work). We will now consider each of the three terms in the context of the Fc-D SAM structures.

Since the same potential changes were applied to Fc-D(**1**) and Fc-D(**2**) modified surfaces, the surface charging effect ($\Delta\sigma$) is expected to be constant and so this factor is unlikely to contribute to their different behaviors. The motion of ions into and out of the film intrinsically affects the refractive index (Δn) at the interface and, thus, the SPR angular changes. Besides, the redox properties of ferrocene moieties were found to be dependent on the nature of the anions in solution [45]. However, this could not explain the different behavior observed for Fc-D(**1**) and Fc-D(**2**) modified surfaces, since the permeation of ions through both films is expected to be the same. Changes in the thickness of the film (Δd) are also expected to promote the SPR angle shift, and this is likely the dominant factor explaining the different behavior. Indeed, oxidation of the ferrocene moiety yields cationic ferricinium, which is electrostatically driven as far away as possible from the positively charged gold surface, thus increasing the apparent film thickness, as observed previously in the reorganization of ferrocenyl alkyl thiol monolayers [44]. Because the alkyl chain of Fc-D(**2**) is longer than that of Fc-D(**1**), where the ferrocene units are directly tethered to the dendrimer, if the alkyl chain becomes more perpendicular to

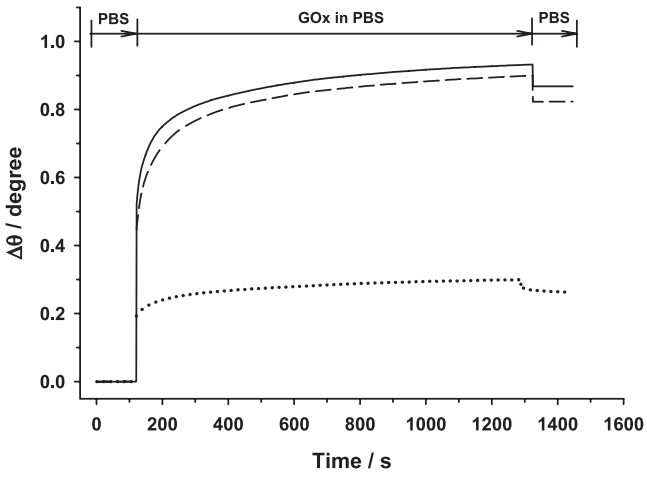

Figure 3. SPR sensorgrams for the binding interaction of periodate-oxidized GOx to the AUT SAM surface (dotted line) and to Fc-D modified MUA SAM surfaces with the short (**1**, dashed line) and long (**2**, solid line) alkyl chain. Measurements were performed in a 0.1 M phosphate buffer solution (PBS) at pH = 6.8.

the gold substrate surface the change in the thickness of the Fc-D(**2**) film will be larger than that of the Fc-D(**1**) film; then the SPR dip shift of the Fc-D(**2**) modified MUA SAM surface will be bigger than that observed for the Fc-D(**1**) modified electrode. The analysis of the scan rate on the SPR dip shift of the ferrocenyl-tethered dendrimer confirms this hypothesis. Conversely, if compared to Fc-D(**1**) film, the SPR dip shifts for the Fc-D(**2**) film gradually decrease when the scan rate changes from 0.05 to 0.300 V s^{-1} (figure 2, inset); this is consistent with a kinetic limitation on the orientation of the ferrocene moieties. By increasing the scan rate there is no enough time for the alkyl chains of Fc-D(**2**) to change their tilt angle and the film thickness. That is the higher the scan rate, the shorter the time for the Fc-D(**2**) film to change orientation, and this results in a decrease in the SPR signal.

Since the SPR monitors the change in refractive index of the medium immediately next to the gold sensing surface, this optical technique was also used in preliminary experiments to confirm the immobilization of GOx onto the modified gold surface. In the resulting sensorgram plots shown in figure 3, the mass of bound protein is proportional to the difference between the SPR baseline signal before injection of the protein and the signal after reinjection of the wash buffer [46, 47].

The above spectroscopic behavior, obtained after incubation for 20 min of periodate-oxidized GOx upon the Fc-D modified surface, confirms the irreversible assembly of the hybrid system, suggesting the formation of Schiff bases between amine groups of the partially modified dendrimers and carbaldehyde groups of periodate-oxidized GOx. A complete and homogeneous immobilization of the GOx over the coated gold surface can be evidenced from the fact that another injection of a higher concentration of the protein showed only a small increase in the resonance angle. Preliminary SPR investigations were also performed to determine whether the use of a dendrimer layer significantly improves the protein immobilization yield on a gold surface. For this purpose we compared the Fc-D modified MUA SAM surface and an unmodified AUT SAM surface. As evidenced in figure 3, a three-fold enhancement of signal intensity was obtained by using both dendrimer modified surfaces (**1** or **2**) when compared with the AUT-only surface. Taking into account the average GOx diameter of about 67 ± 5 Å, a densely packed monolayer of GOx (as expected for the AUT SAM surface) exhibits a surface coverage of the enzyme corresponding to about 4.5×10^{-12} mol cm^{-2} [48]. Thus, the surface coverage of GOx on the Fc-D modified electrode was estimated to be 13.5×10^{-12} mol cm^{-2}. This greater protein immobilization efficiency could be ascribed to a net increase in the total surface accessible area that accompanies the binding of Fc-D particles to the sensor surface and the particular three-dimensional steric arrangement of the large number of amino groups available for covalent coupling that is present on each dendrimer surface.

Figure 4(A) shows the bioelectrocatalytic currents generated by the integrated GOx-Fc-D(**2**) system in the presence of different glucose concentrations. Electrochemical oxidation of the ferrocene units to ferrocenyl cations results in the mediated oxidation of the $FADH_2$ site of GOx and the subsequent oxidation of glucose. As the concentration of glucose is increased, the electrocatalytic anodic current is enhanced; a linear relation between the current response of the electrode and the content of glucose in the concentration range 0.7–15 mM was observed. The anodic current density levels off at a concentration higher than 30 mM to a maximum value of $I^{sat} = 187.5\ \mu A\ cm^{-2}$. From the saturation anodic current density and from the surface coverage of the enzyme molecules, we estimated the turnover rate of electrons transferred to the electrodes to be about 143.9 electrons s^{-1}. Control experiments revealed that the ferrocene units were essential for mediating the bioelectrocatalytic oxidation of glucose, since the immobilization of GOx on dendrimer modified MUA SAM electrode did not lead to any electrocatalytic currents. Figure 4(B) describes the cyclic voltammograms corresponding to the analysis of different concentrations of glucose by the integrated GOx-Fc-D(**1**) modified MUA SAM electrode; a low intensity electrocatalytic current is observed. The amperometric responses at $E = 0.4$ V versus SCE of the GOx-Fc-D(**2**) integrated system toward the analysis of glucose are up to 3.8-fold higher than the current responses generated by GOx-Fc-D(**1**) modified electrode (figure 4(C)). The lower current obtained with the integrated GOx-Fc-D(**1**) modified electrode, as compared to the GOx-Fc-D(**2**) system, may be attributed to the immobilized protein that is poorly electronically coupled to the electrode so that the electron transfer rate is too low for a considerable bioelectrocatalytic current to be observed. A deep investigation of the interconnection between redox chemistry and catalytic activity was performed by EC-SPR. In the presence of glucose $\Delta\theta$ shows the same potential dependence as in the absence of glucose. Therefore the effect of the redox state of the enzyme and glucose on $\Delta\theta$ was far less than that of the mediator film; under controlled potential conditions, the surface concentration ratio of the two redox states of the mediator was determined by electrode potential. As the redox state of the mediator changes, the rearrangement of the ions (ion transport), to maintain

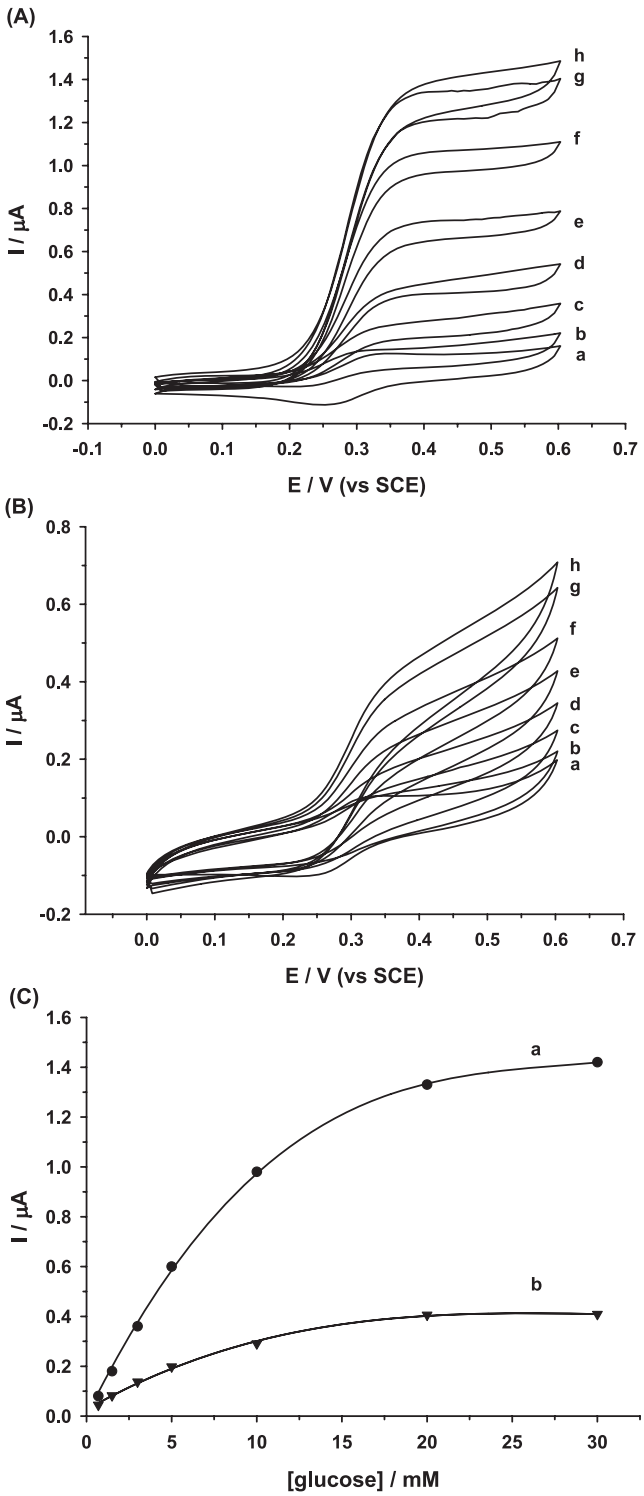

Figure 4. Cyclic voltammograms corresponding to the electrocatalytic anodic current generated by the integrated GOx-Fc-D modified MUA SAM surfaces with the long (**2**, A) and short (**1**, B) alkyl chains in the presence of different concentrations of glucose (mM): 0.0 (a), 0.7 (b), 1.5 (c), 3.0 (d), 5.0 (e), 10.0 (f), 20.0 (g) and 30.0 (h). Data were recorded in 50 mM Tris-HCl buffer pH 7.2 and 50 mM KCl, under N_2 at room temperature, and potential scan rate 0.01 V s^{-1}. (C) Calibration curve corresponding to the electrocatalytic current measured at $E = 0.4$ V versus SCE at variable concentration of glucose using the GOx integrated electrode with Fc-D(**2**) (curve a) and Fc-D(**1**) (curve b).

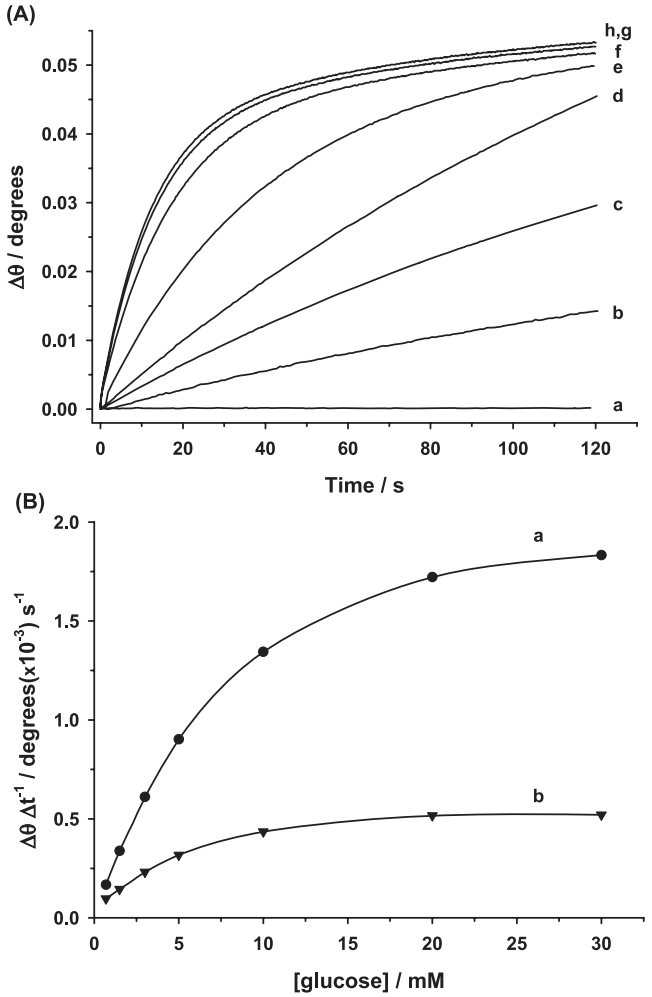

Figure 5. (A) Time course of the SPR signal ($\Delta\theta$) in the chronopotentiometry of the integrated GOx Fc-D(**2**) modified MUA SAM gold electrode in the presence of different concentrations of glucose (mM): 0.0 (a), 0.7 (b), 1.5 (c), 3.0 (d), 5.0 (e), 10.0 (f), 20.0 (g) and 30.0 (h). The measurements were performed in 50 mM Tris-HCl buffer pH 7.2 and 50 mM KCl, under N_2 at room temperature, by setting the electrode potential at 0.6 V. (B) Comparison of the slope of $\Delta\theta$ obtained at variable concentrations of glucose using the GOx integrated electrode with Fc-D(**2**) (curve a) and Fc-D(**1**) (curve b).

charge neutrality, induces a refractive index change, and the results of this transport are directly reflected in $\Delta\theta$. Thus the SPR signal could be monitored in a potentiometric experiment, setting the potentiostat in the electrometer mode. The electrode potential was held at 0.6 V before each substrate addition. At time 0, the mediator was fully oxidized by the electrochemical reaction because the potential was set far higher than the redox potential of the mediator. In the presence of glucose, the $\Delta\theta$ decreases because the oxidized ferrocene was reduced by sequential reaction of GOx (figure 5(A)). The amplitude of $\Delta\theta$ between two redox states was always the same, confirming that the sensitivity of the substrate concentration did not depend on the refractive index of the substrate. The slope of the SPR signal ($\Delta\theta\,\Delta t^{-1}$) was steeper at higher glucose concentrations (figure 5(B)). Comparison of the magnitudes of the sensitivity of the Fc-D(**2**) and Fc-D(**1**) biosensors reveals that the signal is

about 3.6-fold higher for Fc-D(**2**), confirming our hypothesis regarding the higher electron coupling of the ferrocene units tethered through a long alkyl chain between the electrode and the enzyme. Thus, the EC-SPR approach can conveniently deduce the dynamics of the Fc-D SAM reorganization process and their involvement in the biocatalyzed transformations.

The final aspect to consider relates to the stability of the resulting integrated enzyme electrodes. The bioelectrocatalytic activity of the integrated system lost $<10\%$ of its activity within 1 week. The electrode reveals an activity decrease of $\sim 5\%$ upon continuous operation at room temperature for 12 h. This stability seems to be due to the structural integrity of the assembled system, which is a result of the multiple covalent linkages formed between biological molecules and dendrimers and also of the rigidity of the dendrimers as building blocks.

4. Conclusions

In this study we have addressed the characterization of ferrocenyl-tethered dendrimers on a SAM coated surface. The co-assembled units provide binding sites for covalent attachment of the enzyme, to yield an integrated, electrically contacted bioelectrocatalytic assembly.

In situ electrochemical SPR measurements enabled us to transduce the bioelectrocatalytic functions of the enzyme modified film by amperometric or optical means.

Moreover, the EC-SPR technique enabled us to study the different aspects of the redox-induced film thickness changes, ion-pair formation, and hydration. An understanding of the physical change of the co-assembled structure brought about by the applied potential is fundamental for developing an efficient biosensor interface.

Besides the demonstration that the integrated hybrid system exhibits controlled and improved sensing capabilities, the significance of this study is focused on the design of a new composite material that controls the biosensing performance. Because the integration of the SAM with dendrimers is an appealing choice in nanofabrication techniques, the assembly of these materials with enzymes facilitate the downscaling of biosensors to the nanometer regime.

Acknowledgments

Work carried out with the financial support of the University of Rome ‘La Sapienza’ and of the European Commission under contract no. 017350 (BioMedNano).

References

[1] Bartlett P N 2008 *Bioelectrochemistry: Fundamentals, Experimental Techniques and Applications* (Weinheim: Wiley–VCH)
[2] Léger C and Bertrand P 2008 *Chem. Rev.* **108** 2379–438
[3] Willner I 2002 *Science* **298** 2407–8
[4] Willner I and Katz E 2000 *Angew. Chem. Int. Edn* **39** 1180–218
[5] Wang J 2008 *Chem. Rev.* **108** 814–25
[6] Willner I, Yan Y-M, Willner B and Tel-Vered R 2009 *Fuel Cells* **1** 7–24
[7] Cracknell J A, Vincent K A and Armstrong F A 2008 *Chem. Rev.* **108** 2439–61
[8] Holt R E and Cotton T M 1989 *J. Am. Chem. Soc.* **111** 2815–21
[9] Bartlett P N, Tebbutt P and Whitaker R G 1991 *Prog. React. Kinet.* **16** 55–155
[10] Schumann W, Ohara T J, Schmidt H-L and Heller A 1991 *J. Am. Chem. Soc.* **113** 1394–7
[11] Willner I, Riklin B, Shoham D and Rivenzon E 1993 *Adv. Mater.* **5** 912–5
[12] Anicet N, Anne A, Moiroux J and Savéant J-M 1998 *J. Am. Chem. Soc.* **120** 7115–6
[13] Gregg B A and Heller A 1991 *J. Phys. Chem.* **95** 5970–5
[14] Wang Y, Joshi P P, Hobbs K L, Johnson M B and Schmidtke D W 2006 *Langmuir* **22** 9776–81
[15] Raitman O A, Katz E, Bückman A F and Willner I 2002 *J. Am. Chem. Soc.* **124** 6487–96
[16] Xiao Y, Patolsky F, Katz E, Hainfeld J F and Willner I 2003 *Science* **299** 1877–81
[17] Fruk L, Kuo C-H, Torres E and Niemeyer C M 2009 *Angew. Chem. Int. Edn* **48** 2–27
[18] Kavangh P and Leech D 2006 *Anal. Chem.* **78** 2710–6
[19] Cosnier S, Innocent C and Jouanneau Y 1994 *Anal. Chem.* **66** 3198–201
[20] Bosman A W, Jensen E W and Meijer E W 1999 *Chem. Rev.* **99** 1665–72
[21] Tomalia D A 2005 *Prog. Polym. Sci.* **30** 294–310
[22] Astruc D, Ornelas C and Ruiz J 2008 *Acc. Chem. Res.* **41** 841–59
[23] Amatore C, Grun F and Maisonhaute E 2003 *Angew. Chem. Int. Edn* **42** 4944–8
[24] Ornelas C, Ruiz J, Belin C and Astruc D 2009 *J. Am. Chem. Soc.* **131** 590–2
[25] Oh S-K, Baker L A and Crooks R M 2002 *Langmuir* **18** 6981–6
[26] Yoon H C, Hong M-Y and Kim H-S 2000 *Anal. Chem.* **72** 4420–7
[27] Nijhuis C A, Boukamp B A, Ravoo B J, Huskens J and Reinhoudt D N 2007 *J. Phys. Chem.* C **111** 9799–810
[28] Appoh F E, Long Y-T and Kraatz H-B 2006 *Langmuir* **22** 10515–22
[29] Love J C, Estroff L A, Kriebel J K, Nuzzo R G and Whiteside G M 2005 *Chem. Rev.* **105** 1103–69
[30] Tokuhisa H, Liu J L, Omori K, Kanesato M, Hiratani K and Baker L A 2009 *Langmuir* **25** 1633–7
[31] Knoll W 1998 *Annu. Rev. Phys. Chem.* **49** 569–638
[32] Sriwichai S, Baba A, Deng S, Huang C, Phanichphant S and Advincula R C 2008 *Langmuir* **24** 9017–23
[33] Wain A J, Do H N L, Mandal H S, Kraatz H-B and Zhou F 2008 *J. Phys. Chem.* C **112** 14513–9
[34] Iwasaki Y, Horiuchi T and Niwa O 2001 *Anal. Chem.* **73** 1595–8
[35] Zaborsky O R and Ogletree J 1974 *Biochem. Biophys. Res. Commun.* **61** 210–6
[36] Cang-Rong J T and Pastorin G 2009 *Nanotechnology* **20** 255102–21
[37] Gardner T J, Frisbie C D and Wrighton M S 1995 *J. Am. Chem. Soc.* **117** 6927–33
[38] Kretschmann E 1971 *Z. Phys.* **241** 313–24
[39] Katz E, Schlereth D D and Schmidt H-L 1994 *J. Electroanal. Chem.* **367** 59–70
[40] Savéant J-M 2006 *Elements of Molecular and Biomolecular Electrochemistry* (Hoboken: Wiley–Interscience)
[41] Laviron E 1979 *J. Electroanal. Chem.* **101** 19–28
[42] Boussaad S, Pean J and Tao N J 2000 *Anal. Chem.* **72** 222–6
[43] Zhai P, Guo J, Xiang J and Zhou F 2007 *J. Phys. Chem.* C **111** 981–6
[44] Yao X, Wang J, Zhou F, Wang J and Tao N 2004 *J. Phys. Chem.* B **108** 7206–12
[45] Ju H and Leech D 1999 *Phys. Chem. Chem. Phys.* **1** 1549–54
[46] Sigal G B, Mrksich M and Whitesides G M 1998 *J. Am. Chem. Soc.* **120** 3464–73
[47] Chen X, Ferrigno R, Yang J and Whitesides G M 2002 *Langmuir* **18** 7009–15
[48] Bourdillon C, Cueris J, Moiroux J and Savéant J-M 1993 *J. Am. Chem. Soc.* **115** 12264–9